The American Journal of Pathology, Vol. 175, No. 1, July 2009

DOI: 10.2353/ajpath.2009.081001

Molecular Pathogenesis of Genetic and Inherited Diseases

Decreased Catalase Expression and Increased Susceptibility to Oxidative Stress in Primary Cultured Corneal Fibroblasts from Patients with Granular Corneal Dystrophy Type II

Seung-il Choi,* Tae-im Kim,*† Kyu Seo Kim,‡ Bong-Yoon Kim,*† So-yeon Ahn,* Hyun-ju Cho,* Hyung Keun Lee,*† Hyun-Soo Cho,§ and Eung Kweon Kim*†

From the Corneal Dystrophy Research Institute, and Department of Ophthalmology, Yonsei University College of Medicine, Seoul, Korea; the BK21 Project Team of Nanobiomaterials for Cell-based Implants,† Yonsei University, Seoul, Korea; the Department of Chemistry,‡ Duke University, Durham, North Carolina; and the Department of Biology,§ College of Life Science and Biotechnology, Yonsei University, Seoul, Korea*

Granular corneal dystrophy type II (GCD II) is an autosomal dominant disorder characterized by age-dependent progressive accumulation of transforming growth factor-β-induced protein (TGFBIp) deposits in the corneal stroma. Several studies have suggested that corneal fibroblasts may decline with age in response to oxidative stress. To investigate whether oxidative stress is involved in the pathogenesis of GCD II, we assayed antioxidant enzymes, oxidative damage, and susceptibility to reactive oxygen species-induced cell death in primary cultured corneal fibroblasts (PCFs) from GCD II patients and healthy subjects. We found elevated protein levels of Mn-superoxide dismutase, Cu/Zn-superoxide dismutase, glutathione peroxidase, and glutathione reductase, as well as increased *CAT* mRNA and decreased catalase protein in GCD II PCFs. Furthermore, catalase is down-regulated in normal PCFs transfected with transforming growth factor-β-induced gene-h3. We also observed an increase in not only intracellular reactive oxygen species and H_2O_2 levels, but also malondialdehyde, 4-hydroxynonenal, and protein carbonyls levels in GCD II PCFs. Greater immunoreactivity for malondialdehyde was observed in the corneal tissue of GCD II patients. In addition, we observed a decrease in Bcl-2 and Bcl-xL levels and an increase in Bax and Bok levels in GCD II PCFs. Finally, GCD II PCFs are more susceptible to H_2O_2-induced cell death. Together, these results suggest that oxidative damage induced by decreased catalase is involved in GCD II pathogenesis, and antioxidant agents represent a possible treatment strategy. *(Am J Pathol 2009, 175:248–261; DOI: 10.2353/ajpath.2009.081001)*

The cornea, made up of avascular tissue that maintains transparency at the frontal surface of the eye,[1] contains three major layers: the outer epithelium, a thick stroma with corneal fibroblasts, and the inner endothelium. Corneal tissue is chronically exposed to environmental oxidative stimuli such as solar UV radiation and high levels of oxygen,[2] and is known to be particularly susceptible to oxidative stress.[3] For example, the number of corneal fibroblasts declines in normal corneas with age in response to oxidative stress.[4,5]

Reactive oxygen species (ROS) form as products under normal physiological conditions due to the partial reduction of molecular oxygen in mitochondria.[5,6] Eukaryotic cells also have several antioxidative defense mechanisms, including enzymes and antioxidants.[6] There are five major types of primary intracellular antioxidant enzymes: Cu/Zn-superoxide dismutase (SOD), Mn-SOD, catalase, glutathione peroxidase (GPx), and glutathione reductase (GR). The SODs convert O_2^- into H_2O_2, while catalase and GPx convert H_2O_2 into H_2O.[6] Reactive oxygen species (ROS) can be generated at elevated rates under normal aging and pathophysiological conditions.[5,6] Oxidative stress occurs due to excessive ROS production, an impaired antioxidant

Supported by a grant of the Korea Healthcare Technology R&D Project, Ministry for Health, Welfare & Family Affairs, Republic of Korea (A080320).

Accepted for publication April 14, 2009.

Supplemental material for this article can be found on *http://ajp.amjpathol.org.*

Address reprint requests to Eung Kweon Kim, M.D., Ph.D., Department of Ophthalmology, and The Corneal Dystrophy Research Institute, Yonsei University, College of Medicine, #134 Shinchon-dong, Seodaemun-ku, 120-752, Seoul, Korea. E-mail: eungkkim@yuhs.ac.

system, or a combination of these factors.[5,7–9] Excessive ROS can cause oxidative damage to proteins, lipids, and DNA. There are several markers of oxidative damage, including 8-hydroxy-2-deoxyguanosine (8-OHdG, a marker of oxidative damage to DNA), malondialdehyde (MDA, a marker of lipid peroxidation), 4-hydroxynonenal (4-HNE, a marker of lipid peroxidation), and protein carbonyl groups (a marker of protein oxidation). Cell death induced by oxidative stress is involved in the pathologies of various diseases[1,10] including cataract,[11] glaucoma,[12,13] Alzheimer's disease,[14,15] Parkinson's disease,[16,17] and prion disease.[18,19] Furthermore, oxidative cell stress is a common phenomenon in protein misfolding diseases.[20,21] Aggregated forms of many amyloidogenic proteins are toxic to cells via oxidative stress, linking protein aggregation and pathological damage to the tissues in which they are found.[20,21]

Granular corneal dystrophy type II (GCD II) is autosomal dominant disorder caused by point mutations (R124H) in transforming growth factor-β-induced gene-h3 (*BIGH3*). Age-dependent progressive accumulation of hyaline and amyloid are hallmarks of GCD II, which is characterized by the production of transforming growth factor-β-induced protein (TGFBIp) encoded by *BIGH3* in the corneal epithelia and stroma, interfering with corneal transparency.[22–24] TGFBIp is an extracellular matrix protein that is incorporated into deposits in the three major forms of dominant corneal dystrophy caused by different mutation loci in the *BIGH3* gene: the granular type (types I and II; type II is also called Avellino corneal dystrophy), the lattice type (lattice corneal dystrophy types I, III, and IV), and the type with diffuse deposits in Bowman's layer (Reis Buehler corneal dystrophies and Thiel Behnke corneal dystrophy).[23] However, it has not been investigated so far in the context of the worldwide frequency of these disorders. Recently, it has only been reported that 22 homozygous GCD II patients have been found in South Korea.[25] From these results, the frequency of GCD II has been estimated to be 1/1400 in the population of South Korea (manuscript in submission).

Recently, we reported that mitomycin C induces more apoptosis in primary cultured corneal fibroblasts (PCFs) from GCD II patients than wild-type PCFs via reduced *Bcl-xL* and increased *Bax* gene expression.[26] Mitomycin C induces ROS generation through redox cycling.[27,28] Taken together, these data suggest that GCD II PCFs are highly susceptible to ROS-induced cell death, as compared with wild-type PCFs. Therefore, in the present study, we investigated the involvement of oxidative stress in corneal fibroblast degeneration in GCD II by measuring the extent of oxidative damage and the status of the antioxidant enzyme defensive system of PCFs from heterozygous or homozygous GCD II patients and wild-type subjects.

Materials and Methods

Isolation and Culture of PCFs

PCFs were prepared from healthy corneas from the eye bank and from heterozygote or homozygote GCD II patients after penetrating or lamellar keratoplasty. Donor confidentiality was maintained according to the Declaration of Helsinki and was approved by Severance Hospital IRB Committee (CR04124), Yonsei University. GCD II was diagnosed by DNA sequencing analysis of *BIGH3* gene mutations. Age, gender, and diagnosis for all GCD II cases used in this study are listed in Table 1. Corneas were washed three times with Dulbecco's modified Eagle's medium (DMEM; Gibco BRL, Grand Island, NY) containing 1000 units/ml penicillin and 1.0 mg/ml streptomycin sulfate (Gibco BRL, Grand Island, NY). The corneal epithelium was then removed by scraping the epithelial surface and detaching Descemet's membrane with a fine forceps and blade. Corneal tissues were placed on 30-mm culture dishes and DMEM containing 1000 units/ml penicillin, 1.0 mg/ml streptomycin sulfate, and 10% fetal bovine serum (Invitrogen-Life Technologies) was added gently. After 48 hours, migratory fibroblasts from the corneal button could be found. These PCFs were maintained in DMEM with 10% fetal bovine serum at 37°C under 95% humidity and 5% CO_2. The medium was changed every 3 days. When the cultured corneal fibroblasts were ~80% to 90% confluent, the cells were subcultured with 0.25% trypsin and 5.0 mmol/L EDTA at a 1:3 split. Cells from passages 5 to 8 were used in the experiments. The normal human corneal fibroblast cell line[29] was kindly provided by Dr. James Jester and were cultured in DMEM with 10% fetal bovine serum at 37°C in a humidified incubator with 95% air and 5% CO_2.

Table 1. Cases Used for Analysis in This Study

Case no.	Pathological diagnosis	Sex	Age	Mean age
1	CON-WT	F	20	
2	CON-WT	M	10	26.25
3	CON-WT	M	29	
4	CON-WT	M	46	
5	GCD II-HE	F	37	
6	GCD II-HE	F	20	32.50
7	GCD II-HE	M	24	
8	GCD II-HE	M	49	
9	GCD II-HO	F	27	
10	GCD II-HO	M	10	
11	GCD II-HO	F	13	20.2
12	GCD II-HO	F	29	
13	GCD II-HO	M	22	

CON-WT, control case; GCD II-HE, heterozygote of granular corneal dystrophy type II case; GCD II-HO, homozygote of granular corneal dystrophy type II case; F, female; M, male.

Preparation of Small Interfering RNA and Transfection

RNA interference (RNAi) oligoribonucleotides corresponding to the following cDNA sequences were purchased from Santa Cruz (Santa Cruz Biotechnology, Santa Cruz, CA): 5′-CCACTAGTCTGACTGATGA-3′ for the human *CAT* gene. Cells were cultured in DMEM at 37°C in 5% CO_2 atmosphere. The 0.5-nmol small interfering RNA (siRNA) were transfected by lipofectamine 2000 (Invitrogen). The media were supplemented with 10% fetal bovine serum (Invitrogen Life Technologies),

penicillin (100 U/ml), and streptomycin sulfate (100 μg/ml; Invitrogen Life Technologies). Cells were then cultured in growth medium for 48 hours before further analysis.

RNA Isolation and Reverse Transcription-PCR

For amplification of *BIGH3*, *CAT*, and *β-actin*, total RNA was isolated from control wild-type, heterozygous, and homozygous PCFs by extraction in TRIZOL Reagent (Invitrogen Life Technologies, Carlsbad, CA). cDNA synthesis and DNA amplification was performed by using the SuperscriptTM One-Step reverse transcription (RT)-PCR System (Invitrogen Life Technologies, Carlsbad, CA) and primers specific for *BIGH3* (forward primer, 5′-GTGTGTGCTGTGCAGAAGGT-3′; reverse primer, 5′-TTGAGAGTGGTAGGGCTGCT-3′), *CAT* (forward primer, 5′-ATCTCGTTGGAAATAACACC-3′; reverse primer, 5′-AGAAACCTGATGCAGAGACT-3′), and *β-actin* (forward primer, 5′-GGACTTCGAGCAAGAGATGG-3′; reverse primer, 5′-AGCACTGTGTTGGCGTACAG-3′), respectively.

BIGH3 cDNA Cloning

Wild-type and mutant *BIGH3* cDNAs were obtained by RT-PCR from total RNA isolated from wild-type or homozygous PCFs by using forward (5′-CACCATGGCGCTCTTCGTGC-3′) and reverse (5′-CTAATGCTTCATCCTCTCTA-3′) oligonucleotides. These cDNAs were subcloned into pcDNA 3.1 vector (Invitrogen Life Technologies, Carlsbad, CA). The resulting plasmids were sequenced in both directions to check the orientation of the insert.

Cell Viability

PCFs were plated in 96-well plates at 10,000 cells/well overnight. Cell proliferation was determined using the CellTiter 96 AQueous One Solution Reagent Cell Proliferation Assay Kit using the tetrazolium compound (3-[4,5-dimethylthiazol-2-yl]-5-(3-carboxymethoxyphenyl)-2-[4-sulfophenyl]-2H- tetrazolium, inner salt; MTS) (Cat. No. G3580; Promega, Madison, WI). Briefly, the culture medium was removed and then 20 μl of MTS solution was added to each well in 100 μl of culture medium. The cultures were incubated at 37°C for 2 to 4 hours under 95% humidity and 5% CO_2. Optical density was measured with a plate reader with a filter setting at 450 nm (reference filter setting, 690 nm).

Fluorescence-Activated Cell Sorting Analysis

Annexin V fluorescence-activated cell sorting (FACS) analysis was performed according to the manufacturer's protocol (Annexin V Fluorescent *in situ* apoptosis detection kit, BioBud Company, Seoul, Korea). Approximately 1×10^4 cells/well were plated into 100 mm^2 tissue culture dishes (Becton Dickinson, NJ). On day 0, the medium was replaced with fresh medium. On day 2, the medium was replaced with medium containing 100 or 200 μmol/L H_2O_2 and harvested after 6 hours. Cells were accutase-treated and washed with PBS pH 7.4 (Cat. No. 10010; Invitrogen Life Technologies, Carlsbad, CA), and 1×10^6 cells were resuspended in 100 μl annexin V incubation buffer and incubated for 15 minutes at room temperature in the dark. A total of 400 μl of 1× binding buffer was added to each sample and the samples were analyzed on a FACS Calibur flow cytometer (Becton-Dickinson Immunocytometry Systems, San Jose, CA).

Preparation of Cell Lysates and Western Blot Analysis

Cell lysates from PCFs were prepared in radio-immunoprecipitation assay buffer (RIPA buffer; 150 mmol/L NaCl, 1% NP-40, 0.5% deoxycholate, 0.1% SDS, 50 mmol/L Tris-HCl, pH 7.4) containing a protease inhibitor tablet (Complete Mini Protease Inhibitor Tablet, Roche # 1836170). Crude cell lysates were centrifuged at 10,000 × *g* for 10 minutes at 4°C to remove nuclear fragments and tissue debris. A portion of the supernatant was used to determine the total protein concentration with a bicinchoninic acid kit (Pierce). Total cellular proteins were electrophoresed in 10% Tris-glycine SDS polyacrylamide gels. Proteins were transferred onto polyvinylidene difluoride membranes (Millipore Corp., Bedford, MA), blocked in 5% dry milk in TBS-T (0.02 mol/L Tris/0.15 mol/L NaCl, pH 7.5 containing 0.1% Tween 20) at room temperature for 1 hour, washed three times with TBS-T and then incubated with primary antibodies to TGFBIp (0.2 μg/ml; Cat. No. AF2935; R&D System), Cu/Zn-SOD (1:1000 dilution; Cat. No. SOD100; Stressgen, Victoria BC, Canada), Mn-SOD (1:1000 dilution; Cat. No. SOD110; Stressgen, Victoria BC, Canada), catalase (1:500 dilution; Cat. No. ab1877, Abcam, Cambridge, UK), GPx (1:250 dilution; Cat. No. LF-PA0087; AbFrontier, Seoul, Korea), GR (1:5000 dilution; Cat. No. LF-PA0087; AbFrontier, Seoul, Korea), β-actin (1:5000 dilution; Cat. No. A-5441; Sigma Chemical Co., St. Louis, MO), or LC3 (1:1000 dilution; Cell Signaling Technology, Beverly, MA) for overnight at 4°C. Pro-survival (Cat. No. #9941) and pro-apoptosis (Cat. No. #9942) Bcl-2 family antibody sampler kits (Cell Signaling Technology Inc., Beverly, MA) were used to analyze apoptosis-related proteins. After washing three times with TBS-T, the blots were incubated with secondary antibodies conjugated with horseradish peroxidase at room temperature for 1 hour. Horseradish peroxidase-linked anti-mouse IgG (1:5000 dilution; Cat. No. NA931V) or anti-rabbit IgG (1:5000 dilution; Cat. No. NA934V) was used as a secondary antibody (Amersham Pharmacia Biotech., Piscataway, NJ). Immunoblots were visualized using the enhanced chemiluminescence system (Pierce; Rockford, IL). The intensities of immunoreactive protein bands were image-scanned and optical densities of the bands were quantified using computer software (ImageJ software, version 1.37, Wayne Rasband, NIH), corrected by background subtraction and normalized to the intensity of the corresponding β-actin protein bands.

Antioxidant Enzyme Activity Assay

Cells were homogenized in ice-cold KCl buffer (0.3 M/L KCl, 0.15 M/L K_2HPO_4, 10 mmol/L $Na_4P_2O_7$, 1 mmol/L $MgCl_2$ [pH 6.8]) and centrifuged at 10,000 $\times$ *g* for 10 minutes at 4°C. Protein concentrations of the supernatants were measured by the bicinchoninic acid protein assay (Pierce BCA-200 Protein Assay kit; Rockford, IL). SOD activity was determined with the SOD Assay Kit-WST (Dojindo Inc., Kumamoto, Japan) in PCFs from the rate of reduction of cytochrome c, with 1U of SOD activity defined as the amount of SOD required to inhibit the rate of cytochrome c reduction by 50%. SOD activity was expressed as U/mg protein. Catalase activity was assayed by monitoring the loss of absorbency of H_2O_2 at 240 nm; 1U was the amount of enzyme that decomposed 1 mmol/L H_2O_2/min.[30]

Measurement of Intracellular ROS and H_2O_2 Generation

Dichlorofluorescein diacetate (DCF-DA; Sigma Chemical Co., St. Louis, MO) was dissolved in ethanol to a final concentration of 20 mmol/L before use. Cells were washed twice with PBS to remove endogenous esterase activity in the FBS. To measure ROS, cells were incubated with 10 mmol/L DCF-DA at 37°C for 30 minutes. Extracellular DCF-DA was removed by washing twice with PBS. The fluorescence intensity was recorded using a fluorescent microplate reader (HTS 7000, Perkin-Elmer Corp., Norwalk, CT) with an excitation filter of 485 nm and an emission filter of 535 nm. To measure intracellular H_2O_2, cells were washed twice with PBS and then incubated with 5 mmol/L BES-H_2O_2 (Wako Pure Chemical Co., Osaka, Japan) at 37°C for 60 minutes. Extracellular BES-H_2O_2 was removed by washing twice with PBS. The fluorescence intensity was recorded using a luminescence spectrometer (LS50B, Perkin-Elmer Corp., Norwalk, CT) with an excitation filter of 485 nm and an emission filter of 515 nm. Data were calculated as the percentage of fluorescence intensity of wild-type control cultures.

Analysis of MDA, 4-HNE, and Protein Carbonyl Group Levels

The level of protein carbonyl groups as markers of oxidized protein in GCD II PCFs patients was determined using an OxyBlot protein oxidation detection kit (Cat. No. S7150; Chemicon, Temecula, CA) according to the manufacturer's protocol. Briefly, whole cell extracts were analyzed for protein oxidation by derivatization of protein carbonyls with 2, 4-dinitrophenyl hydrazine by Western blotting using anti-2,4-dinitrophenyl hydrazine antibody (1:150 dilutions). After determining the protein content of each fraction, equal amounts of protein were separated by 10% Tris-Tricin SDS-polyacrylamide gel electrophoresis, followed by Western blot transfer to polyvinylidene difluoride membranes (Millipore Corp., Bedford, MA), and visualized by chemiluminescence. Proteins that underwent carbonyl group formation were assayed as a band in the samples derivatized with 2,4-dinitrophenyl hydrazine. The same samples were processed for detection of 4-HNE and MDA adducts by immunoblotting using anti-4-HNE (1:500 dilution; Cat. No. 4-HNE11-S; Alpha Diagnostic, San Antonio, TX) and anti-MDA (1:500 dilution; Cat. No. MDA11-S; α Diagnostic, San Antonio, TX) polyclonal antibodies developed against 4-HNE- and MDA-adducted proteins (Alpha Diagnostic, San Antonio, TX). Blots were analyzed using ImageJ analysis software (version 1.37, Wayne Rasband, NIH).

Immunocytochemical Staining

Wild-type, heterozygous, and homozygous PCFs grown on culture slides (Cat. No. REF 354108; BD Falcon, Labware, Franklin Lakes, NJ) were permeabilized and fixed in methanol at 20°C for 3 minutes. Cells were washed in PBS, blocked with 10% bovine serum albumin (Sigma) in PBS for 10 minutes, and incubated with primary antibody in blocking buffer for 1 hour at 37°C. Cells were incubated with secondary antibodies for 1 hour at 37°C. The coverslips were mounted on glass slides with Vectashield mounting medium (Vector Labs Inc., Burlingame, CA). Cells were viewed under a Leica TCS SP5 confocal microscope (Leica). The following primary antibodies were used: monoclonal anti-TGFBIp (1:300 dilution; kindly provided by Dr. IS, Kim, Kyungpook National University, Korea), polyclonal anti-catalase (1:500 dilution; Cat. No. ab1877, Abcam, Cambridge, UK), and anti-LAMP2 mouse monoclonal antibody, H4B4 (purchased from Developmental Studies Hybridoma Bank at the University of Iowa). The following secondary antibodies were used: an Alexa 594 (red)-conjugated anti-rabbit IgG (1:200 dilution; Vector Laboratories) and fluorescein isothiocyanate (green)-labeled anti-mouse IgG (1:200 dilution; Jackson ImmunoResearch Laboratories, West Grove, PA).

Immunohistochemical Staining

Immunohistochemical procedures were performed using the ABC kit (Vector Labs Inc., Burlingame, CA) with a modification of the avidin-biotin-peroxidase method. Briefly, 6-μm sections of cornea were dewaxed with xylene and hydrated with graded ethanol, and then treated with 0.3% H_2O_2 in methyl alcohol for 20 minutes to block endogenous peroxidase. After washing three times with PBS, the sections were exposed to normal goat serum, and then incubated overnight at 4°C with anti-TGFBIp (KE-2, 1:50 dilution, kindly provided by Dr. Daniel F. Schorderet, University of Lausanne, Switzerland) and anti-MDA polyclonal antibodies (α Diagnostic, San Antonio, TX, Cat. No. MDA11-S, 1:500 dilution). After washing three times with PBS, the sections were sequentially treated with biotinylated anti-rabbit/mouse immunoglobulin and avidin-biotin peroxidase complex, and developed with diaminobenzidine-hydrogen peroxidase solution (0.003% 3,3-diaminobenzidine and 0.03% hydrogen peroxidase in 0.05 M/L Tris buffer).

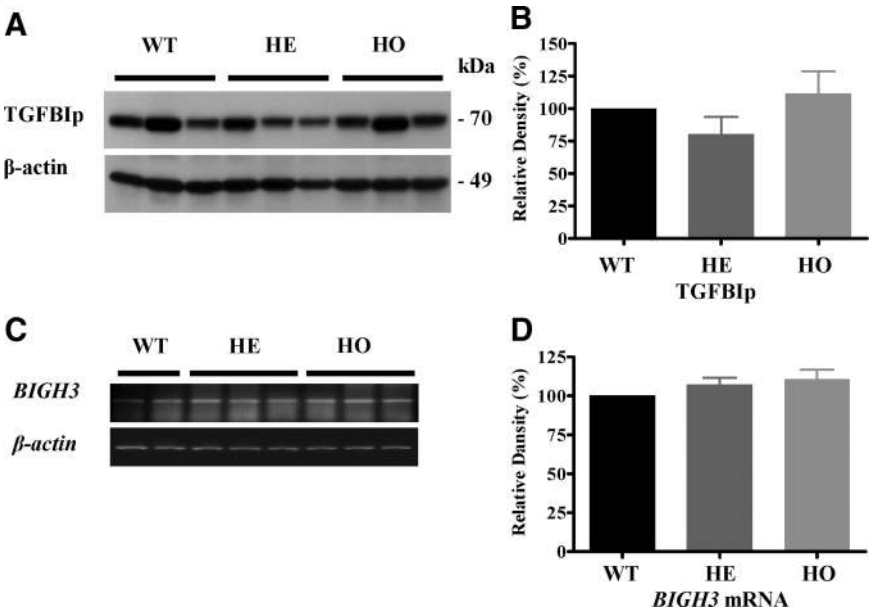

Figure 1. *BIGH3* gene and TGFBIp expression in GCD II PCFs. **A:** Immunoblot analysis of TGFBIp expression among three wild-type (Table 1, samples 1–3), three heterozygous (Table 1, samples 5–7), and three homozygous (Table 1, samples 9–11) PCFs, using anti-TGFBIp polyclonal goat antibodies. Numbers on the **right** correspond to the molecular weight markers in kilodaltons (kDa). **B:** Quantification of TGFBIp in wild-type, heterozygote, and homozygote PCFs. Western blot shows no significant variations among wild-type, heterozygote, and homozygote PCFs. **C:** RT-PCR analysis of *BIGH3* gene expression among two wild-type, three heterozygote, and three homozygote PCFs, using human *BIGH3* gene specific primers. **D:** Quantification of *BIGH3* mRNA in wild-type, heterozygote, and homozygote PCFs. All signals were quantified by using a NIH image J. Heterozygote (HE) or Homozygote (HO) versus control wild-type (WT) cultures.

Statistical Analysis

The results were statistically evaluated for significance ($P < 0.05$) with one-way analysis of variance followed by Newman-Keuls multiple comparison tests. Results are expressed as mean ± SD. All data were processed using the Graph Pad Prism version 4.0 (Graph Pad Software Inc, San Diego, CA) statistical package.

Results

Expression of TGFBIp and BIGH3 Gene in Wild-Type and GCD II PCFs

We have investigated the expression level of TGFBIp in wild-type, heterozygous, and homozygous PCFs. As shown in Figure 1, no significant differences in expression levels of TGFBIp and *BIGH3* mRNA were detected between wild-type, heterozygous, and homozygous PCFs by Western blot (Figure 1, A and B) and RT-PCR (Figure 1, C and D), respectively. The molecular weight of the mutant TGFBIp was similar to that of the wild-type TGFBIp (~70 kDa) (Figure 1A).

Increased Expression of Antioxidant Enzymes in GCD II PCFs

To find out whether oxidative stress is involved in the degeneration of GCD II PCFs, we investigated the expression levels of antioxidant enzymes in heterozygous, homozygous, and wild-type PCFs. As shown in Figure 2, the expression of both Cu/Zn-SOD and Mn-SOD was significantly higher in heterozygous and homozygous PCFs (Figure 2, A–C). Moreover, PCFs homozygous for the mutation displayed a greater elevation of Mn-SOD expression than heterozygous PCFs (Figure 2, A and C). To determine whether the protein level of SOD corresponded to the activity level of enzymes directly involved in ROS scavenging, we measured the total SODs activity from PCF homogenates. Total SOD activity was significantly higher in GCD II PCFs, as compared with wild-type PCFs (Table 2). In addition, to investigate other antioxidant defensive enzymes, we analyzed glutathione-related enzymes by Western blot analysis. GPx (Figure 2, A and D) and GR (Figure 2, A and E) protein expression was markedly higher in heterozygous and homozygous PCFs. Taken together, these results indicate that GCD II PCFs are under oxidative stress.

GCD II PCFs Exhibit Increased CAT mRNA Expression Levels but Decreased Catalase Protein Levels

We found that the level of *CAT* mRNA was significantly higher in GCD II PCFs than wild-type PCFs (Figure 3, C and D). Interestingly, the expression level of catalase protein in both heterozygous and homozygous PCFs was dramatically lower than in wild-type PCFs (Figure 3, A and B). To determine whether the catalase protein level corresponded to the activity level of enzymes directly involved in ROS scavenging, we measured catalase activities in PCF homogenates. Catalase activity was significantly lower in GCD II PCFs than wild-type PCFs (Table 2). In addition, to confirm the lower catalase protein level in GCD II PCFs, we analyzed the distribution of catalase protein by confocal immunostaining. Weak immunoreactivity of catalase was observed in GCD II PCFs (Figure 3, E–J).

Intracellular Generation of ROS and H_2O_2 Increased More in GCD II PCFs than Wild-Type PCFs

To test whether intracellular ROS are elevated in GCD II PCFs under differential expression of antioxidant en-

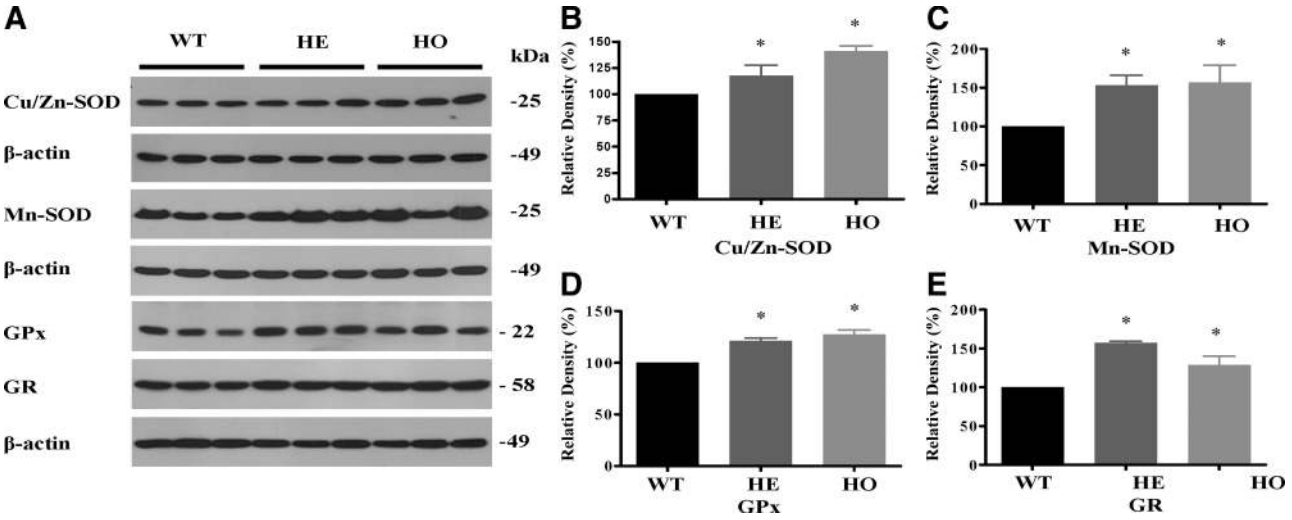

Figure 2. Antioxidative enzymes are elevated in GCD II PCFs. Immunoblot analysis of antioxidant enzymes expression among three wild-type (WT) (Table 1, samples 1–3), three heterozygous (HE) (Table 1, samples 5–7), and three homozygous (HO) (Table 1, samples 9–11) PCFs. **A:** Equal protein amounts of whole cell extracts were analyzed by Western blotting using antibodies directed against Cu/Zn-SOD, Mn-SOD, GPx, and GR. Bands corresponding to Cu/Zn-SOD (**B**), Mn-SOD (**C**), GPx (**D**), and GR (**E**) were quantified using ImageJ software and normalized to β-actin. Molecular size markers are indicated at the **right**. Values are the mean ± SD of three independent experiments. Statistical analysis was performed by one-way analysis of variance, followed by Newman–Keuls multiple comparison test. $^{*}P < 0.05$; $^{**}P < 0.01$.

zymes, intracellular ROS levels were measured by 2′,7′-dichlorodihydrofluorescein (DCFH2-DA) following the oxidation of DCFH2-DA to fluorescent dichlorofluorescein (DCF), which detects the generation of intracellular ROS. As shown in Figure 4A, significantly higher ROS levels were detected in both heterozygous (2.3-fold) and homozygous (8.6-fold) PCFs, as compared with wild-type PCFs. To assess the elevation of H_2O_2 accurately, we also used BES-H_2O_2, a probe for cell-derived H_2O_2 based on a nonoxidative fluorescence mechanism with high selectivity to H_2O_2. The intracellular H_2O_2 level was elevated significantly in both heterozygous (3.7-fold) and homozygous (4.0-fold) PCFs, as compared with wild-type PCFs (Figure 4B). There were no significant differences between heterozygous and homozygous PCFs.

Altered Antioxidant Enzyme Expression and Accumulation of H_2O_2 by siRNA-Mediated Suppression of CAT Gene

The decreased catalase prompted us to further investigate its potential role in this catalase in oxidative stress in GCD II PCFs. We used the siRNA technique to specifically suppress expression of catalase in normal corneal fibroblast cell lines[29] and then examined possible alterations in cellular ROS content and antioxidant enzyme expression. *CAT* siRNA specifically suppressed expression of catalase and did not affect the expression of β-actin (see supplemental Figure S1 at *http://ajp.amjpathol.org*). Next, because GPx also detoxifies H_2O_2 by catalyzing its decomposition to O_2 and H_2O, we analyzed expression levels of GPx after suppression of catalase gene expression by siRNA. Expression levels of GPx are markedly induced in corneal fibroblast cell lines transfected with *CAT* siRNA, whereas the control siRNA did not cause any significant changes in β-actin level (see supplemental Figure S1 at *http://ajp.amjpathol.org*). These data suggest that suppression of catalase expression was sufficient to cause an accumulation of H_2O_2 in PCFs, and may support that catalase is a key factor in oxidative damage in GCD II PCFs. Compared with non-transfected GCD II PCFs, negative control of *CAT* siRNA transfected had slightly reduced catalase expression and induced ROS, which may reflect the side effects of control siRNA transfection.

Oxidative Damage in PCFs and Corneal Tissues of GCD II Patients

Both altered expression of antioxidant enzymes and increased ROS and H_2O_2 levels are expected to lead to

Table 2. Total SOD and Catalase Activities in Wild-Type (Table 1, samples 1–3), Heterozygous (Table 1, samples 5–7), and Homozygous (Table 1, samples 9–11) PCFs

Enzymes	WT	HE	HO
Total SOD activity	36.17 ± 7.46	50.83 ± 5.41*	57.58 ± 5.91*
Catalase activity	0.04947 ± 0.0018	0.01723 ± 0.00025*	0.01833 ± 0.0029*

Results were calculated in units of activity per mg of total protein. One unit of SOD activity was defined as the enzyme activity required to inhibit the production of formazan by 50%. One U was the amount of catalase that decomposed 1 mmol/L H_2O_2/min. Values are the mean ± SD of two or three independent cultures with three replicates each. Statistical analysis was performed by one-way ANOVA, followed by Newman-Keuls multiple comparison test.

$^{*}P < 0.05$, heterozygote (HE) or homozygote (HO) versus wild-type (WT) cultures.

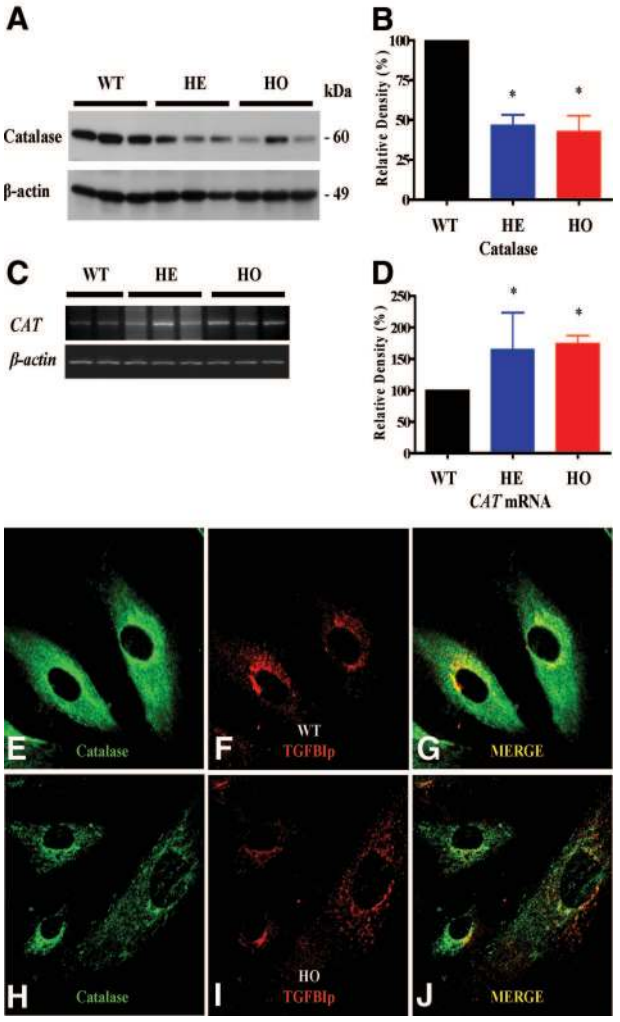

Figure 3. Expression of catalase protein is reduced while *CAT* mRNA is elevated in GCD II PCFs. **A:** Immunoblot analysis of catalase expression among three wild-type (WT) (Table 1, samples 1–3), three heterozygous (HE) (Table 1, samples 5–7), and three homozygous (HO) (Table 1, samples 9–11) PCFs. **B:** Expression level of catalase is significantly reduced in heterozygotes and homozygotes, as compared with wild-type PCFs. **C** and **D:** RT-PCR data indicate that the level of *CAT* mRNA was significantly higher in heterozygotes and homozygotes as compared with wild-type PCFs. **E–J:** The subcellular localization of catalase and TGFBIp in homozygous and wild-type PCFs. Immunostaining for catalase was less intense in homozygous (**H:** Table 1, sample 10) than wild-type (**E:** Table 1, sample 1) PCFs. Magnification = ×60. Molecular size markers are indicated at the **right**. Values are the mean ± SD of three independent experiments. Statistical analysis was performed by one-way analysis of variance, followed by Newman–Keuls multiple comparison test. $^{**}P < 0.01$, heterozygous or homozygous versus wild-type cultures.

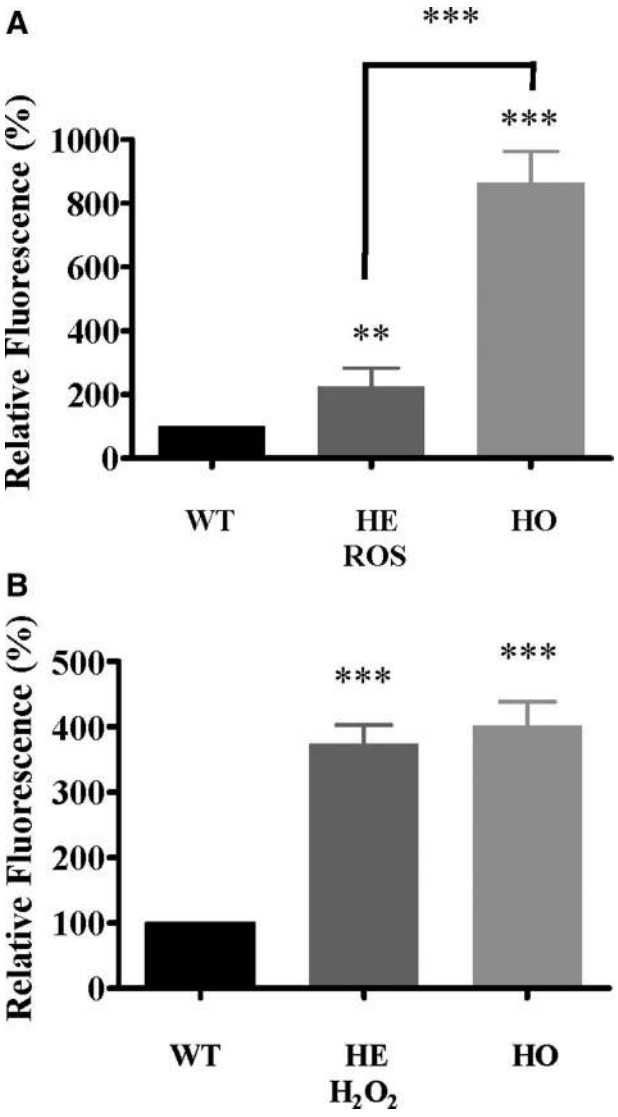

Figure 4. Generation of ROS and H_2O_2 elevation in GCD II PCFs. Wild-type (WT) (Table 1, samples 2–3), heterozygous (HE) (Table 1, samples 6–7), and homozygous (HO) (Table 1, samples 9–10) PCFs were incubated with 2′, 7′-dichloro-fluorescein (DCF) and BES-H_2O_2 for 30 minutes and the levels of ROS and H_2O_2 were determined as described in *Materials and Methods*. Generation of ROS (**A**) and H_2O_2 (**B**) was significantly higher in heterozygous and homozygous PCFs, as compared with wild-type PCFs. Values are the mean ± SD of at least three independent experiments. Statistical analysis was performed by one-way analysis of variance, followed by Newman–Keuls multiple comparison test. $^{***}P < 0.001$ heterozygous or homozygous versus wild-type cultures.

oxidative damage. Accordingly, we estimated oxidative damage by quantifying levels of the lipid peroxidation products, MDA and 4-HNE, and we quantified protein oxidative damage using protein carbonyl formation as a marker. The levels of protein carbonyl groups (Figure 5A), MDA (Figure 5B), and 4-HNE (Figure 5C) were significantly elevated in GCD II PCFs compared with wild-type PCFs. Next, to confirm oxidative damage in corneal tissues of GCD II patients, we investigated the distribution of MDA using immunohistochemical staining. As shown in Figure 5, D–G, MDA immunoreactivity was detectable in the epithelial cells of corneal tissue from both age-matched normal controls and GCD II patients. In contrast, stronger immunoreactivity of MDA was observed in the corneal stroma and epithelia of GCD II patients (Figure 5, F and G), as compared with age-matched normal corneal tissue (Figure 5, D and E). In addition, immunostaining of corneal tissues showed a positive reaction with TGFBIp specific antibody (KE-2) in all examined samples (Figure 5, H–K). These results also revealed that mutant TGFBIp is a major component of corneal deposits (Figure 5, J and K). In corneal stroma, typical fusiform deposits of different sizes showed intense staining with the specific KE-2 antibody (Figures 5, J and K). TGFBIp staining was also noticed within the cytoplasm of epithelial cells.

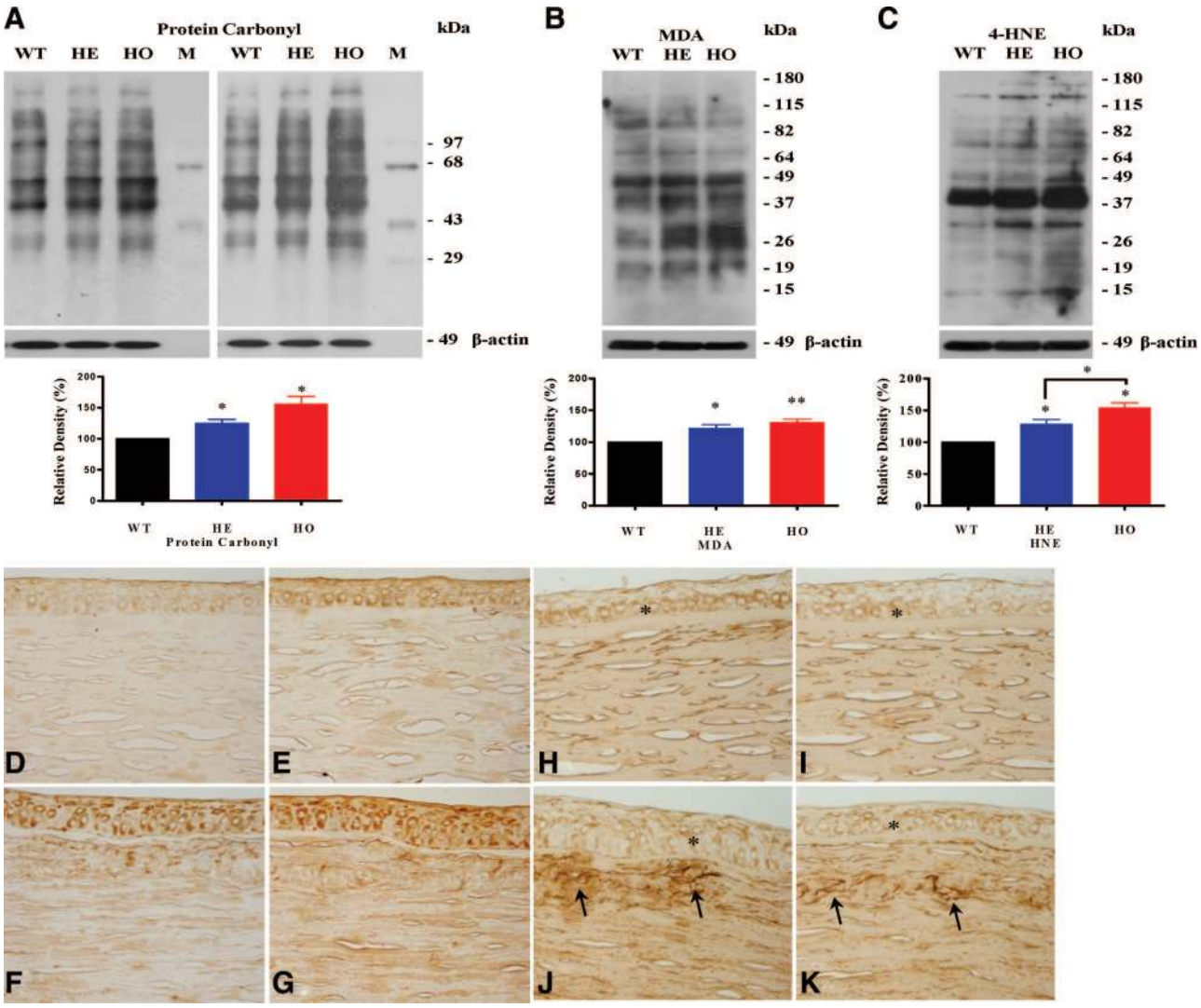

Figure 5. Immunoblot analyses of carbonylated proteins, MDA, and 4-HNE in between GCD II and wild-type (WT) PCF, and immunohistochemical staining for MDA and TGFBIp in corneal tissue. Levels of carbonylated proteins in PCF extracts were determined with an OxyBlot Protein Oxidation Detection Kit. Western blotting for oxidatively modified proteins using anti-dinitrophenylhydrazone demonstrated a significant difference between wild-type controls and GCD II PCFs. Densitometric evaluation of the Western blots showed significant differences in protein carbonyl (**A**), MDA (**B**), and 4-HNE (**C**) between wild-type and GCD II PCFs (Table 1, samples 2–6, 11–12). Corneal tissues of a homozygote GCD II patient (**F** and **G**) show strong immunoreactivity to MDA (Table 1, samples 7 and 13). In a normal aged-matched cornea (**D** and **E**, Table 1, sample 4), MDA immunoreactivity was present in the cytoplasmic compartments of epithelial cells. The corneal stroma also displayed diffused MDA immunoreactivity. In a GCD II cornea (**F** and **G**, Table 1, samples 13–14), strong MDA immunoreactivity was present in the cytoplasmic compartments of most epithelial cells (EP) as well as the stromal matrix (ST). The immunohistochemical staining for TGFBIp is most prominent in epithelial cells (**asterisk**). TGFBIp deposits (**arrows**) are shown on the stroma of corneal tissue (**J** and **K**): normal (**H** and **I**, Table 1 sample 1) and homozygote cornea (**J** and **K**, Table 1, sample 13). Molecular size markers are indicated at the **right**. Values are the mean ± SD of three independent experiments. Statistical analysis was performed by one-way analysis of variance, followed by Newman–Keuls multiple comparison test. $^{*}P < 0.05$; $^{**}P < 0.01$, heterozygous (HE) or homozygous (HO) versus wild-type cultures. Magnification = original ×200.

Catalase is Down-Regulated in Wild-Type PCFs Transfected with BIGH3 Gene

To investigate whether mutant *BIGH3* (*BIGH3-R124H*) expression in wild-type cells induces heterozygous PCF-like properties, we transfected wild-type PCFs with a plasmid containing the *BIGH3-R124H* or the *BIGH3* gene. Surprisingly, catalase was significantly decreased in PCFs transfected with *BIGH3-R124H* as well as *BIGH3* (Figure 6, A and B). Furthermore, catalase expression decreased more in PCFs transfected with *BIGH3-R124H* than in PCFs transfected with *BIGH3* (Figure 6, A and B). In addition, because catalase and GPx are physiologically involved in the elimination of H_2O_2, to determine whether these cells compensate for their ROS burdens induced by decreased catalase, we assayed expression of various antioxidant enzymes in cells transfected with the *BIGH3* and *BIGH3-R124H* genes. We found that levels of Cu/Zn-SOD, Mn-SOD, GPx, and GR expression showed an increase in cells transfected with *BIGH3-R124H* or *BIGH3* (Figure 6A). Furthermore, these levels tended to be slightly increased in cells transfected with *BIGH3-R124H* (Figure 6A). This result is the first evidence that TGFBIp could regulate catalase expression. Increased antioxidant enzymes also revealed that cells compensate for their increased ROS burdens by de-

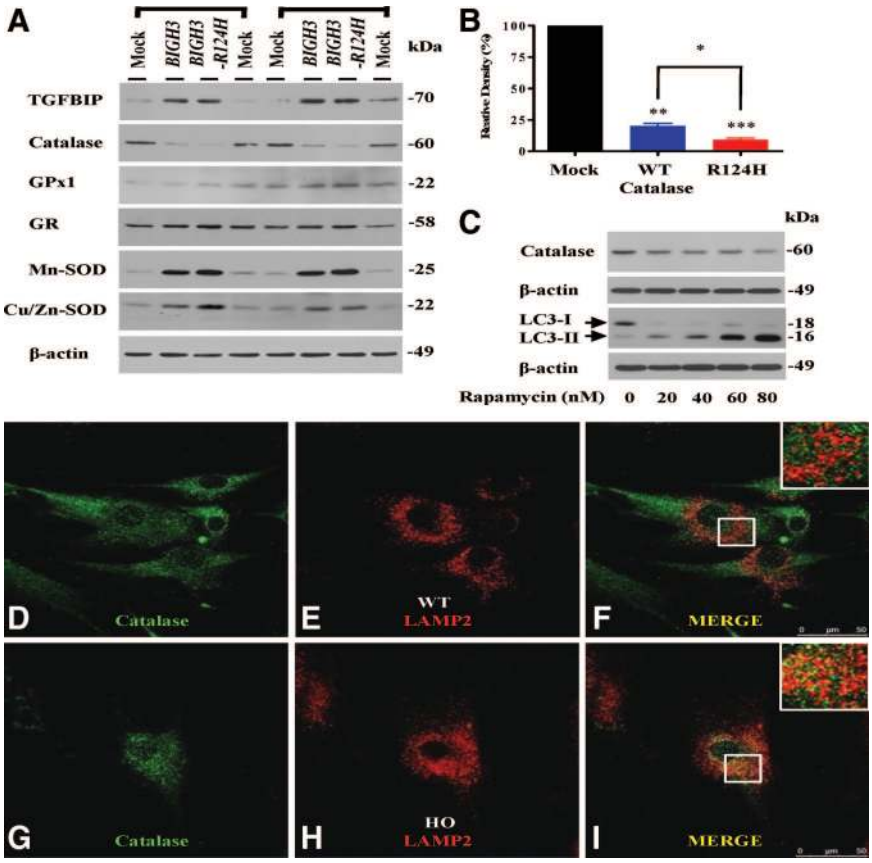

Figure 6. Expression levels of catalase and other antioxidants enzymes in normal PCFs transfected with *BIGH3* genes. **A:** Wild-type (WT) PCFs (Table 1, samples 3 and 4) were either transfected with wild-type *BIGH3*, mutant *BIGH3* (R124H), or nontransfected (Mock). Cells were harvested 48 hours after transfection. Proteins (25 μg) were analyzed by Western blotting. Actin was used as a loading control. Catalase level is down-regulated in wild-type PCFs transfected with *BIGH3* or *BIGH3–R124H* gene. **B:** The amount of catalase is decreased significantly in *BIGH3–R124H* transfectants compared with *BIGH3* transfectants. Values are the mean ± SD of three independent experiments. **C:** Catalase level is decreased in the normal human corneal fibroblast cell line treated with autophagy inducer, rapamycin. After exposure to rapamycin for 12 hours, cell lysates were subjected to Western blot analysis using an antibody against LC3 and catalase. An anti-β-actin antibody was used to confirm equal loading of proteins. **D–I:** Catalase is present inside the lysosomal compartment in GCD II PCFs. PCFs cells were fixed, permeabilized, blocked, and stained with catalase-specific antibody (**D** and **G:** green), or LAMP-2 (**E** and **H:** red) antibody. The secondary antibodies were conjugated with either fluorescein isothiocyanate or Alexa 594. Cells were viewed with a confocal microscope. Green fluorescence for catalase stain, red fluorescence for lysosomal stain (LAMP-2), and the merged images (MERGE) are shown. Colocalization is indicated by yellow. Magnification = original ×60.

creased catalase. Next, because it has been reported that catalase is targeted to the lysosomes for degradation during autophagy,[31,32] to assess whether the decrease in catalase is involved in autophagic degradation, we treated a normal human corneal fibroblast cell line[29] with an autophagy inducer, rapamycin. It has been well known that increased LC3-II protein indicates generation of autophagy. LC3-II protein increased in cells treated with rapamycin in a dose-dependent manner (Figure 6C), and catalase level dramatically decreased in cells treated with rapamycin in a dose-dependent manner (Figure 6C). In addition, to explore whether catalase is targeted to the lysosomal compartment for degradation, we monitored catalase localization by confocal microscopy in homozygous and wild-type PCFs. Catalase was colocalized with the lysosomal marker protein LAMP-2 in homozygous PCFs (Figure 6, G–I) but not in wild-type PCFs (Figure 6, D–F). These results suggest that decreased catalase is involved in autophagic degradation.

CAT Gene Polymorphisms Are Not Involved in Reduced Catalase Protein Levels in GCD II PCFs

In many cases, polymorphisms of genes leading to a reduction of protein and mRNA stability have been postulated to be a possible mechanism. The human catalase gene consists of 13 exons and is located on chromosome 11p13.[33] Several rare mutations/polymorphisms have been reported in the catalase gene, most of them being associated with acatalasemia. Therefore, to determine whether the genetic basis is associated with reduced catalase level, we investigated a mutation and polymorphism in structural gene and promoter of *CAT* gene from the samples used in this study. However, we did not find any polymorphism or mutation in *CAT* genes from normal and GCD II patients (data not shown). These observations suggest that the reduction of catalase expression in GCD II PCFs is not due to a marked mutant or polymorphism of *CAT* gene. However, larger sample sizes, intron, and the 5′- and 3′-untranslated region of *CAT* gene need further investigation. Primers and PCR conditions for specific amplification of *CAT* gene are provided in supplementary Table S1 (see *http://ajp.amjpathol.org*).

Differential Expression of Cell Death- and Survival-Related Proteins in GCD II PCFs

Because ROS-induced oxidative damages result in cell death, we analyzed the expression levels of apoptosis-related proteins. The expression of Bcl-2 (Figure 7, A and B) and Bcl-xL (Figure 7, A and C) was significantly lower in heterozygous and homozygous PCFs, as compared with wild-type PCFs, while the expression of Bax (Figure 7, A and D) and Bok (Figure 7, A and E) proteins was significantly higher in GCD II PCFs.

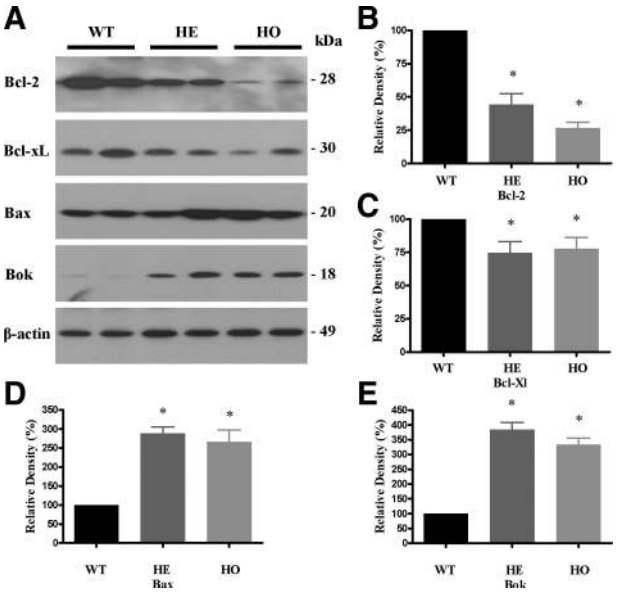

Figure 7. Differential expression of cell death- and survival-related proteins. Levels of Bcl-2, Bcl-xL, Bax, and Bok were detected by immunoblotting in the cell lysates of wild-type and GCD II PCFs. **A:** Equal amounts (50 μg) of protein from each sample were immunoblotted with anti-Bcl-2, anti-Bcl-xL anti-Bax, anti-Bok, and anti-β-actin antibodies. A statistically significant decrease in Bcl-2 (**B**) and Bcl-xL (**C**) and increase in Bax (**D**) and Bok (**E**) was detected in GCD II PCFs (Table 1, samples 6–11), as compared with wild-type PCFs (Table 1, samples 2–4). Values are the mean ± SD of three independent experiments. Statistical analysis was performed by one-way analysis of variance, followed by Newman–Keuls multiple comparison test. * $P < 0.05$; ** $P < 0.01$; *** $P < 0.001$, heterozygous (HE) or homozygous (HO) versus wild-type cultures. Molecular masses are indicated in kDa.

GCD II PCFs Are More Sensitive to H_2O_2-Induced Cell Death Than Wild-Type PCFs

To further investigate the role of oxidative stress in GCD II, we analyzed the effects elicited by incubating GCD II and wild-type PCFs for 6 hours in the presence of 0, 100, or 200 μmol/L H_2O_2 (Figure 8). First, we performed Annexin-V/PI-FACS analyses to determine whether the observed cell death occurred via the process of apoptosis (Figure 8A). Significantly more H_2O_2-treated cells displayed early morphological events of apoptosis (wild-type: 5.4%; homozygous: 15.2%) in 100 μmol/L treatment and apoptosis (wild-type: 8.3%; homozygous: 17.0%) in 200 μmol/L treatment than untreated cells (wild-type: 2.1%; homozygous: 4.6%) (Figure 8A). Second, we determined cell viability using MTS reduction. The viability of primary cultured heterozygous and homozygous PCFs declined significantly within 6 hours in the presence of various H_2O_2 concentrations compared with wild-type (Figure 8B). After exposure to 100, 150, 200, and 250 μmol/L H_2O_2 for 6 hours, cell viability in wild-type PCFs decreased by about 85.38, 79.75, 71.58, and 50.13%, respectively ($P < 0.05$). In contrast, cell viability in heterozygous PCFs decreased by about 78.96, 64.30, 50.93, and 37.15%, respectively ($P < 0.05$). The cell viability of homozygous PCFs was the most susceptible to H_2O_2, with cell viability reductions of about 63.51, 42.35, 24.66, and 12.19%, respectively ($P < 0.05$).

Discussion

Our results provide the first evidence for the involvement of oxidative stress in the pathogenesis of GCD II. This novel role is supported by the following observations in GCD II PCFs: (1) increased Cu/Zn-SOD, Mn-SOD, GPx, and GR expression, and decreased catalase expression; (2) increased intracellular ROS and H_2O_2 generation; (3) increased 4-HNE, MDA, and protein carbonyl groups content, as well greater MDA immunoreactivity in GCD II corneal tissues; (4) decreased catalase in wild-type PCFs transfected transiently with *BIGH3* gene; (5) decreased Bcl-2 and Bcl-xL expression, and increased Bax and Box expression; and (6) increased susceptibility to oxidative stress-induced cell death.

Aging and age-related or protein aggregation-related diseases appear to have a common type of oxidative

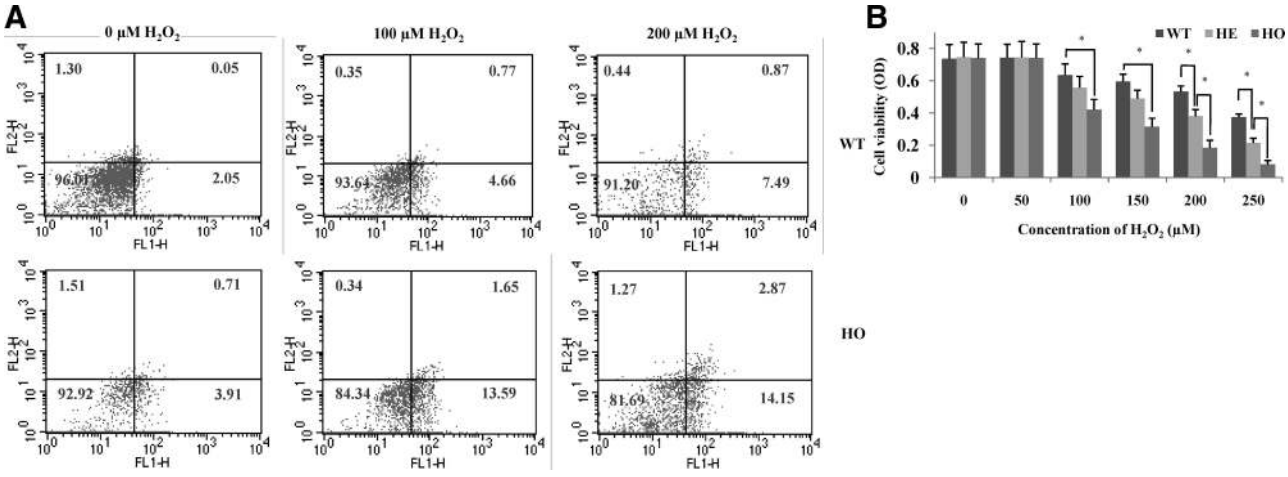

Figure 8. GCD II PCFs are most susceptible to H_2O_2-induced cell death. **A:** Assay of apoptotic cell death by FACS analysis. PI-stained wild-type (WT) (Table 1, sample 1) and homozygous (HO) (Table 1, sample 10) PCFs were FACS-sorted after exposure to 100 μmol/L and 200 μmol/L H_2O_2. A statistically significant increase in apoptotic cells was detected in GCD II PCFs, as compared with control cells. **B:** Cell viability of wild-type (Table 1, samples 1 and 2), heterozygous (HE) (Table 1, samples 5 and 6), and homozygous (Table 1, samples 9–10) PCFs was determined by MTS assay after 6 hours stimulation with various concentration of H_2O_2. Cell viability was calculated by the equation: MTS OD value of sample/MTS OD value of control (cells treated with PBS). Values are the mean ± SD of at least three independent experiments.

damage.[34,35] Because the cornea absorbs approximately 80% of UV B light, it has the greatest potential for elevated ROS generation and/or oxidative stress. GCD II is an autosomal dominant genetic disorder characterized by age-dependent progressive accumulation of TGFBIp deposits in the epithelia and stroma of the cornea.[23,24,36,37] TGFBIp deposits are also involved in the degenerated corneal fibroblasts that are observed in the corneal stroma of GCD.[38] Despite the numerous antioxidant systems in mammalian cells, ROS generation can increase under normal aging and pathophysiological conditions through an altered oxidant-antioxidant status. Several studies have also demonstrated that the aggregated proteins associated with diseases can elevate the generation of ROS, and that the increased ROS may constitute a fundamental mechanism in oxidative damage and cell death. The regulatory responses of antioxidant enzyme genes to oxidative stress have been described.[39] For example, the expression of both Mn-SOD and GPx is induced by ROS, with little change in Cu/Zn-SOD or catalase. Shull et al also demonstrated the greatest induction of catalase expression in response to H_2O_2 and smaller increases in GPx and Mn-SOD expression.[40] These data suggest that the increased levels of both Cu/Zn- and Mn-SOD in GCD II PCFs are dynamic responses to ROS and/or oxidative stress. Similarly, the increase in expression of both GPx and GR may relate to a defensive response to elevated intracellular H_2O_2. Catalase is a major enzyme involved in the detoxification of H_2O_2 from cells, and increased levels of catalase by transcriptional activation can be found in H_2O_2-stressed various cell lines.[41–43] However, the regulation of catalase expression under oxidative stress is not predictable. For example, activity and protein and/or mRNA of catalase are decreased,[44–51] increased,[52–54] or unchanged[55] during oxidative stress. Furthermore, catalase increased at both the mRNA and protein levels with a conformable increase in catalase enzyme activity, but no differences exist in expression of Mn-SOD, CuZnSOD, and GPx.[56] Several studies have also described adaptive regulation of activities of catalase exposure to H_2O_2. In fact, levels of mRNA and protein of catalase are induced by a low concentration of H_2O_2 in human lens epithelial cells.[57] In addition, catalase activities, protein levels, and mRNA levels increased markedly by enhanced mRNA stability of catalase through multiple exposures to a low dose of H_2O_2 in fibroblasts.[58] On the other hand, it has been shown that ceramide treatments induce oxidative damage through proteolytic cleavage of catalase by activated caspase-3. Activated caspase-3 decreased catalase protein levels because of its proteolysis, not because of inhibition of mRNA levels.[59] Finally, cytokines and nitric oxide inhibit enzyme activity of catalase but not its protein or mRNA expression.[60] Although regulation of catalase is complex, in this study, increased mRNA expression of catalase is most easily explained as a response to elevated H_2O_2, because increased H_2O_2 generation was also observed in GCD II PCFs. Furthermore, decreased catalase and increased SODs activities can accelerate H_2O_2 generation by increasing the conversion of O_2^- into H_2O_2, which causes cellular oxidative damage such as lipid peroxidation and/or cell death.[61] Increased MDA (Figure 5B), 4-HNE (Figure 5C), and protein carbonyl group (Figure 5A) levels has been found in GCD II PCFs. These results suggest that decreased catalase and increased SOD expression may be responsible for the excessive oxidative damage in GCD II PCFs. Therefore, reduced catalase activity reveals that corneas of patients with GCD II may suffer from elevated H_2O_2 levels. Furthermore, corneal tissue is chronically exposed to solar UV radiation and high levels of oxygen,[2] and is known to be particularly susceptible to oxidative stress.[3] Taken together, we propose that decreased catalase in GCDII PCFs could make the cornea more susceptible to oxidative stress in corneas of patients with GCD II.

Numerous studies have demonstrated a strong correlation between oxidative stress and apoptosis in different cell types.[61,62] Thus, oxidative stress leads to apoptosis when antioxidant capacity is insufficient.[62] Therefore, these findings provide a possible link between apoptosis and oxidative stress in the degeneration of corneal fibroblasts in GCD II. Previously, the relationship between corneal fibroblasts apoptosis and antioxidant enzymes levels has been also demonstrated in corneal surgeries such as photorefractive keratectomy and laser *in situ* keratomileusis.[63–66] Excimer laser stromal photoablation also induces a decrease in corneal GPx activity,[65] and the apoptosis of corneal fibroblast is induced by decreased GPx activity after corneal epithelial scraping.[66] Furthermore, the low level of H_2O_2 caused by the upregulation of catalase protects against apoptosis.[67] Taken together, we suggest that the heightened susceptibility of GCD II PCFs to H_2O_2-induced cell death may be caused by decreased catalase expression. We also showed that a decline in the anti-apoptotic protein Bcl-2 was involved in the apoptotic cell death of GCD II PCFs. Lower levels of Bcl-2 can disturb its ROS scavenging function,[68] and overexpression of catalase leads to an increase in Bcl-2 expression.[69] By detoxifying ROS, catalase reverses the reduction in Bcl-2 expression caused by oxidative stress and prevents apoptosis. ROS and Bcl-2 levels have a reciprocal relationship,[70] where an increase in ROS correlates with a decrease in Bcl-2 levels and vice versa.[71,72] This finding suggests that increased generation of ROS may lead to a decline in Bcl-2 levels in GCD II PCFs.

There are discrepancies between the mRNA and protein level of catalase in GCD II PCFs. To explain these results, we here propose that the decreased catalase protein level may be due to proteolytic degradation rather than decreased translational activation. Autophagy plays a known role in the degradation of peroxisomes, which are subcellular organelles with a single membrane that contains catalase mainly as a matrix enzyme.[73,74] Li Yu et al demonstrated that autophagy can lead to the degradation of peroxisomal catalase, and the resulting accumulation of ROS in the cell leads to cell death.[31] More recently, we also observed significantly greater autophagy using Western blots for the autophagy marker LC3 in GCD II PCFs, as compared with wild-type PCFs (unpublished data). Furthermore, catalase-positive compartments were frequently colocalized with LAMP-2 in ho-

mozygous PCFs (Figure 6I), but not wild-type PCFs (Figure 6F). These data suggest that catalase is degraded by a lysosomal degradation pathway via autophagic processing. Therefore, we speculate that peroxisomal degradation by autophagy may be involved in the catalase degradation machinery in GCD II PCFs. In addition, several investigations have shown that catalase is regulated by ubiquitination and proteosomal degradation.[75] Recent study has revealed that there is specific autophagic degradation of polyubiquitinated protein aggregates as a clearance mechanism. This study also showed that ubiquitination of both protein and cellular compartments containing peroxisomes are efficiently targeted to autophagosomes, and then degraded in lysosomes. Although we did not detect ubiquitinated catalase in GCD II PCFs, based on these reports, we propose that the ubiquitination of catalase involved in the selective lysosomal targeting of catalase. Finally, because polymorphisms and mutation of genes leading to a reduction of protein and mRNA stability have been postulated to be a possible mechanism, to examine whether mutations and polymorphisms of the *CAT* gene are associated with decreased levels of catalase, we analyzed sequences of 13 exons in the *CAT* gene and its promoter from the blood of patients and controls used in this study (see supplemental Table S1 at *http://ajp.amjpathol.org*). These data suggest that the reduction of catalase expression in GCD II PCFs is not due to a marked mutant or polymorphism of the *CAT* gene. Taken together, although these results reveal that the regulation of catalase has more complex patterns, we consider the possibility that TGFBIp is involved in the regulation of catalase protein.

It is well accepted that ROS can react rapidly with almost all biological substances and induce the peroxidation of lipids and proteins. ROS attacks on macromolecules are another important cause of protein damage, misfolding, and aggregation within cells.[76,77] Notably, protein aggregation is facilitated by partial unfolding during oxidative stress. Therefore, aggregation and accumulation of oxidatively damaged proteins occurs in cells or tissues.[78,79] Oxidative stress can also directly injure corneal tissues by cleaving corneal stromal macromolecules, such as proteoglycans and collagen.[80,81] These studies reveal that corneal tissue damage induced by oxidative stress may be involved in the developmental processing of TGFBIp deposits, because TGFBIp most easily interacts with type I collagen and fibronectin,[82] which can be easily damaged by oxidative stress.[76] Moreover, abnormal collagen and proteoglycan deposits appear in the anterior stroma in GCD.[83] Therefore, we propose that TGFBIp deposits in corneal tissues may be involved in specific associations between oxidatively modified TGFBIp and extracellular matrix (ECM) components. TGFBIp is ECM protein that has four internal repeat domains homologous to the *Drosophila* protein fasciclin-1.[84] The mutation (R124H) in TGFBIp is predicted to alter either protein solubility or stability,[85] and likely affects protein–protein interactions in ECM.[85] Extracellular-SOD also catalyzes the breakdown of O_2^- to H_2O_2 in ECM. This enzyme has high affinity with sulfated glycosaminoglycans and mainly exists anchored to proteoglycans in ECM.[86,87] Because it has been demonstrated that TGFBIp mediates cell adhesion by interacting with various ECM components, such as proteoglycan, collagens, fibronectin, and several integrins,[82,88] we consider that the mutation of TGFBIp may lead to changes in proteoglycan and collagen structure and subsequence it may accelerate the oxidative damage by lack of binding sites of extracellular SOD in the ECM.

The functional significance of the TGFBIp in the cornea is still unclear. Here we suggest that TGFBIp could regulate metabolism of catalase. Although, no interactions between TGFBIp and catalase, as revealed by co-immunoprecipitation assays, have been found (data not shown), this is supported by significantly decreased catalase in PCFs transfected with mutant *BIGH3* or wild-type *BIGH3* and by colocalization between TGFBIp and catalase in cytosolic compartment of PCFs.

In conclusion, the oxidative damage induced by decreased catalase activity may play a pivotal role in the pathogenesis of GCD II, potentially providing a therapeutic intervention strategy that involves antioxidant agents.

Acknowledgments

We thank Dr. Yeong-Min Yoo for critical review of the manuscript.

References

1. Buddi R, Lin B, Atilano SR, Zorapapel NC, Kenney MC, Brown DJ: Evidence of oxidative stress in human corneal diseases. J Histochem Cytochem 2002, 50:341–351
2. Wenk J, Brenneisen P, Meewes C, Wlaschek M, Peters T, Blaudschun R, Ma W, Kuhr L, Schneider L, Scharffetter-Kochanek K: UV-induced oxidative stress and photoaging. Curr Probl Dermatol 2001, 29:83–94
3. Shoham A, Hadziahmetovic M, Dunaief JL, Mydlarski MB, Schipper HM: Oxidative stress in diseases of the human cornea. Free Radic Biol Med 2008, 45:1047–1055
4. Berlau J, Becker HH, Stave J, Oriwol C, Guthoff RF: Depth and age-dependent distribution of keratocytes in healthy human corneas: a study using scanning-slit confocal microscopy in vivo. J Cataract Refract Surg 2002, 28:611–616
5. Finkel T, Holbrook NJ: Oxidants, oxidative stress and the biology of ageing. Nature 2000, 408:239–247
6. Droge W: Free radicals in the physiological control of cell function. Physiol Rev 2002, 82:47–95
7. Lenaz G: Role of mitochondria in oxidative stress and ageing. Biochim Biophys Acta 1998, 1366:53–67
8. Genet S, Kale RK, Baquer NZ: Alterations in antioxidant enzymes and oxidative damage in experimental diabetic rat tissues: effect of vanadate and fenugreek (Trigonellafoenum graecum). Mol Cell Biochem 2002, 236:7–12
9. Tian L, Cai Q, Wei H: Alterations of antioxidant enzymes and oxidative damage to macromolecules in different organs of rats during aging. Free Radic Biol Med 1998, 24:1477–1484
10. Mates JM, Perez-Gomez C, Nunez de Castro I: Antioxidant enzymes and human diseases. Clin Biochem 1999, 32:595–603
11. Spector A, Ma W, Wang RR, Kleiman NJ: Microperoxidases catalytically degrade reactive oxygen species and may be anti-cataract agents. Exp Eye Res 1997, 65:457–470
12. Zanon-Moreno V, Pinazo-Duran MD: Oxidative stress theory of glaucoma. J Glaucoma 2008, 17:508–509
13. Zanon-Moreno V, Marco-Ventura P, Lleo-Perez A, Pons-Vazquez S, Garcia-Medina JJ, Vinuesa-Silva I, Moreno-Nadal MA, Pinazo-Duran MD: Oxidative stress in primary open-angle glaucoma. J Glaucoma 2008, 17:263–268

14. Smith MA, Rottkamp CA, Nunomura A, Raina AK, Perry G: Oxidative stress in Alzheimer's disease. Biochim Biophys Acta 2000, 1502:139–144
15. Butterfield DA, Drake J, Pocernich C, Castegna A: Evidence of oxidative damage in Alzheimer's disease brain: central role for amyloid beta-peptide. Trends Mol Med 2001, 7:548–554
16. Jenner P: Oxidative stress in Parkinson's disease. Ann Neurol 2003, 53 Suppl 3:S26–S36; discussion S36–S28
17. Onyango IG: Mitochondrial dysfunction and oxidative stress in Parkinson's disease. Neurochem Res 2008, 33:589–597
18. Kim JI, Choi SI, Kim NH, Jin JK, Choi EK, Carp RI, Kim YS: Oxidative stress and neurodegeneration in prion diseases. Ann NY Acad Sci 2001, 928:182–186
19. Choi SI, Ju WK, Choi EK, Kim J, Lea HZ, Carp RI, Wisniewski HM, Kim YS: Mitochondrial dysfunction induced by oxidative stress in the brains of hamsters infected with the 263 K scrapie agent. Acta Neuropathol 1998, 96:279–286
20. Squier TC: Oxidative stress and protein aggregation during biological aging. Exp Gerontol 2001, 36:1539–1550
21. Tabner BJ, El-Agnaf OM, German MJ, Fullwood NJ, Allsop D: Protein aggregation, metals and oxidative stress in neurodegenerative diseases. Biochem Soc Trans 2005, 33:1082–1086
22. Skonier J, Neubauer M, Madisen L, Bennett K, Plowman GD, Purchio AF: cDNA cloning and sequence analysis of beta ig-h3, a novel gene induced in a human adenocarcinoma cell line after treatment with transforming growth factor-beta. DNA Cell Biol 1992, 11:511–522
23. Klintworth GK: Advances in the molecular genetics of corneal dystrophies. Am J Ophthalmol 1999, 128:747–754
24. Korvatska E, Henry H, Mashima Y, Yamada M, Bachmann C, Munier FL, Schorderet DF: Amyloid and non-amyloid forms of 5q31-linked corneal dystrophy resulting from kerato-epithelin mutations at Arg-124 are associated with abnormal turnover of the protein. J Biol Chem 2000, 275:11465–11469
25. Moon JW, Kim SW, Kim TI, Cristol SM, Chung ES, Kim EK: Homozygous granular corneal dystrophy type II (Avellino corneal dystrophy): natural history and progression after treatment. Cornea 2007, 26:1095–1100
26. Kim TI, Choi SI, Lee HK, Cho YJ, Kim EK: Mitomycin C induces apoptosis in cultured corneal fibroblasts derived from type II granular corneal dystrophy corneas. Mol Vis 2008, 14:1222–1228
27. Pagano G: Mitomycin C and diepoxybutane action mechanisms and FANCC protein functions: further insights into the role for oxidative stress in Fanconi's anaemia phenotype. Carcinogenesis 2000, 21:1067–1068
28. Pagano G, Degan P, De Biase A, Iaccarino M, Warnau M: Diepoxybutane and mitomycin C toxicity is associated with the induction of oxidative DNA damage in sea urchin embryos. Hum Exp Toxicol 2001, 20:651–655
29. Jester JV, Huang J, Fisher S, Spiekerman J, Chang JH, Wright WE, Shay JW: Myofibroblast differentiation of normal human keratocytes and hTERT, extended-life human corneal fibroblasts. Invest Ophthalmol Vis Sci 2003, 44:1850–1858
30. Beers RF, Jr., Sizer IW: A spectrophotometric method for measuring the breakdown of hydrogen peroxide by catalase. J Biol Chem 1952, 195:133–140
31. Yu L, Wan F, Dutta S, Welsh S, Liu Z, Freundt E, Baehrecke EH, Lenardo M: Autophagic programmed cell death by selective catalase degradation. Proc Natl Acad Sci USA 2006, 103:4952–4957
32. Kim PK, Hailey DW, Mullen RT, Lippincott-Schwartz J: Ubiquitin signals autophagic degradation of cytosolic proteins and peroxisomes. Proc Natl Acad Sci USA 2008, 105:20567–20574
33. Quan F, Korneluk RG, Tropak MB, Gravel RA: Isolation and characterization of the human catalase gene. Nucleic Acids Res 1986, 14:5321–5335
34. Gerster H: Review: antioxidant protection of the ageing macula. Age Ageing 1991, 20:60–69
35. Beckman KB, Ames BN: The free radical theory of aging matures. Physiol Rev 1998, 78:547–581
36. Munier FL, Frueh BE, Othenin-Girard P, Uffer S, Cousin P, Wang MX, Heon E, Black GC, Blasi MA, Balestrazzi E, Lorenz B, Escoto R, Barraquer R, Hoeltzenbein M, Gloor B, Fossarello M, Singh AD, Arsenijevic Y, Zografos L, Schorderet DF: BIGH3 mutation spectrum in corneal dystrophies. Invest Ophthalmol Vis Sci 2002, 43:949–954
37. Streeten BW, Qi Y, Klintworth GK, Eagle RC, Jr., Strauss JA, Bennett K: Immunolocalization of beta ig-h3 protein in 5q31-linked corneal dystrophies and normal corneas. Arch Ophthalmol 1999, 117:67–75
38. Sornson ET: Granular dystrophy of the cornea: an electron microscopic study. Am J Ophthalmol 1965, 59:1001–1007
39. Ho YS, Dey MS, Crapo JD: Antioxidant enzyme expression in rat lungs during hyperoxia. Am J Physiol 1996, 270:L810–L818
40. Shull S, Heintz NH, Periasamy M, Manohar M, Janssen YM, Marsh JP, Mossman BT: Differential regulation of antioxidant enzymes in response to oxidants. J Biol Chem 1991, 266:24398–24403
41. Spitz DR, Elwell JH, Sun Y, Oberley LW, Oberley TD, Sullivan SJ, Roberts RJ: Oxygen toxicity in control and H2O2-resistant Chinese hamster fibroblast cell lines. Arch Biochem Biophys 1990, 279:249–260
42. Hunt CR, Sim JE, Sullivan SJ, Featherstone T, Golden W, Von Kapp-Herr C, Hock RA, Gomez RA, Parsian AJ, Spitz DR: Genomic instability and catalase gene amplification induced by chronic exposure to oxidative stress. Cancer Res 1998, 58:3986–3992
43. Bojes HK, Suresh PK, Mills EM, Spitz DR, Sim JE, Kehrer JP: Bcl-2 and Bcl-xL in peroxide-resistant A549 and U87MG cells. Toxicol Sci 1998, 42:109–116
44. Ohtake T, Kimura M, Nishimura M, Hishida A: Roles of reactive oxygen species and antioxidant enzymes in murine daunomycin-induced nephropathy. J Lab Clin Med 1997, 129:81–88
45. Iqbal M, Athar M: Attenuation of iron-nitrilotriacetate (Fe-NTA)-mediated renal oxidative stress, toxicity and hyperproliferative response by the prophylactic treatment of rats with garlic oil. Food Chem Toxicol 1998, 36:485–495
46. Kinter M, Wolstenholme JT, Thornhill BA, Newton EA, McCormick ML, Chevalier RL: Unilateral ureteral obstruction impairs renal antioxidant enzyme activation during sodium depletion. Kidney Int 1999, 55:1327–1334
47. Nath KA, Grande J, Croatt A, Haugen J, Kim Y, Rosenberg ME: Redox regulation of renal DNA synthesis, transforming growth factor-beta1 and collagen gene expression. Kidney Int 1998, 53:367–381
48. Clerch LB, Wright A, Chung DJ, Massaro D: Early divergent lung antioxidant enzyme expression in response to lipopolysaccharide. Am J Physiol 1996, 271:L949–L954
49. Singh I, Gulati S, Orak JK, Singh AK: Expression of antioxidant enzymes in rat kidney during ischemia-reperfusion injury. Mol Cell Biochem 1993, 125:97–104
50. Cvetkovic T, Vlahovic P, Pavlovic D, Kocic G, Jevtovic T, Djordjevic VB: Low catalase activity in rats with ureteral ligation: relation to lipid peroxidation. Exp Nephrol 1998, 6:74–77
51. Ricardo SD, Ding G, Eufemio M, Diamond JR: Antioxidant expression in experimental hydronephrosis: role of mechanical stretch and growth factors. Am J Physiol 1997, 272:F789–F798
52. Yoshioka T, Bills T, Moore-Jarrett T, Greene HL, Burr IM, Ichikawa I: Role of intrinsic antioxidant enzymes in renal oxidant injury. Kidney Int 1990, 38:282–288
53. Lai CC, Peng M, Huang L, Huang WH, Chiu TH: Chronic exposure of neonatal cardiac myocytes to hydrogen peroxide enhances the expression of catalase. J Mol Cell Cardiol 1996, 28:1157–1163
54. Clerch LB, Iqbal J, Massaro D: Perinatal rat lung catalase gene expression: influence of corticosteroid and hyperoxia. Am J Physiol 1991, 260:L428–L433
55. Nath KA, Croatt AJ, Likely S, Behrens TW, Warden D: Renal oxidant injury and oxidant response induced by mercury. Kidney Int 1996, 50:1032–1043
56. Dieterich S, Bieligk U, Beulich K, Hasenfuss G, Prestle J: Gene expression of antioxidative enzymes in the human heart: increased expression of catalase in the end-stage failing heart. Circulation 2000, 101:33–39
57. Goswami S, Sheets NL, Zavadil J, Chauhan BK, Bottinger EP, Reddy VN, Kantorow M, Cvekl A: Spectrum and range of oxidative stress responses of human lens epithelial cells to H2O2 insult. Invest Ophthalmol Vis Sci 2003, 44:2084–2093
58. Sen P, Chakraborty PK, Raha S: p38 mitogen-activated protein kinase (p38MAPK) upregulates catalase levels in response to low dose H2O2 treatment through enhancement of mRNA stability. FEBS Lett 2005, 579:4402–4406
59. Iwai K, Kondo T, Watanabe M, Yabu T, Kitano T, Taguchi Y, Umehara H, Takahashi A, Uchiyama T, Okazaki T: Ceramide increases oxidative damage due to inhibition of catalase by caspase-3-dependent proteolysis in HL-60 cell apoptosis. J Biol Chem 2003, 278: 9813–9822
60. Sigfrid LA, Cunningham JM, Beeharry N, Lortz S, Tiedge M, Lenzen S, Carlsson C, Green IC: Cytokines and nitric oxide inhibit the enzyme

activity of catalase but not its protein or mRNA expression in insulin-producing cells. J Mol Endocrinol 2003, 31:509–518
61. Stoian I, Oros A, Moldoveanu E: Apoptosis and free radicals. Biochem Mol Med 1996, 59:93–97
62. Yabuki M, Kariya S, Ishisaka R, Yasuda T, Yoshioka T, Horton AA, Utsumi K: Resistance to nitric oxide-mediated apoptosis in HL-60 variant cells is associated with increased activities of Cu, Zn-superoxide dismutase and catalase. Free Radic Biol Med 1999, 26:325–332
63. Shimmura S, Masumizu T, Nakai Y, Urayama K, Shimazaki J, Bissen-Miyajima H, Kohno M, Tsubota K: Excimer laser-induced hydroxyl radical formation and keratocyte death in vitro. Invest Ophthalmol Vis Sci 1999, 40:1245–1249
64. Helena MC, Baerveldt F, Kim WJ, Wilson SE: Keratocyte apoptosis after corneal surgery. Invest Ophthalmol Vis Sci 1998, 39:276–283
65. Yis O, Bilgihan A, Bilgihan K, Yis NS, Hasanreisoglu B: The effect of excimer laser keratectomy on corneal glutathione peroxidase activities and aqueous humor selenium levels in rabbits. Graefes Arch Clin Exp Ophthalmol 2002, 240:499–502
66. Kasetsuwan N, Wu FM, Hsieh F, Sanchez D, McDonnell PJ: Effect of topical ascorbic acid on free radical tissue damage and inflammatory cell influx in the cornea after excimer laser corneal surgery. Arch Ophthalmol 1999, 117:649–652
67. Lin SJ, Shyue SK, Liu PL, Chen YH, Ku HH, Chen JW, Tam KB, Chen YL: Adenovirus-mediated overexpression of catalase attenuates ox-LDL-induced apoptosis in human aortic endothelial cells via AP-1 and C-Jun N-terminal kinase/extracellular signal-regulated kinase mitogen-activated protein kinase pathways. J Mol Cell Cardiol 2004, 36:129–139
68. Hockenbery DM, Oltvai ZN, Yin XM, Milliman CL, Korsmeyer SJ: Bcl-2 functions in an antioxidant pathway to prevent apoptosis. Cell 1993, 75:241–251
69. Hildeman DA, Mitchell T, Aronow B, Wojciechowski S, Kappler J, Marrack P: Control of Bcl-2 expression by reactive oxygen species. Proc Natl Acad Sci USA 2003, 100:15035–15040
70. Pugazhenthi S, Nesterova A, Jambal P, Audesirk G, Kern M, Cabell L, Eves E, Rosner MR, Boxer LM, Reusch JE: Oxidative stress-mediated down-regulation of bcl-2 promoter in hippocampal neurons. J Neurochem 2003, 84:982–996
71. Maulik N, Engelman RM, Rousou JA, Flack JE, 3rd, Deaton D, Das DK: Ischemic preconditioning reduces apoptosis by upregulating anti-death gene Bcl-2. Circulation 1999, 100:369–375
72. Chang WK, Yang KD, Chuang H, Jan JT, Shaio MF: Glutamine protects activated human T cells from apoptosis by up-regulating glutathione and Bcl-2 levels. Clin Immunol 2002, 104:151–160
73. Farre JC, Subramani S: Peroxisome turnover by micropexophagy: an autophagy-related process. Trends Cell Biol 2004, 14:515–523
74. Monastyrska I, Klionsky DJ: Autophagy in organelle homeostasis: peroxisome turnover. Mol Aspects Med 2006, 27:483–494
75. Cao C, Leng Y, Liu X, Yi Y, Li P, Kufe D: Catalase is regulated by ubiquitination and proteosomal degradation. Role of the c-Abl and Arg tyrosine kinases, Biochemistry 2003, 42:10348–10353
76. Grune T, Jung T, Merker K, Davies KJ: Decreased proteolysis caused by protein aggregates, inclusion bodies, plaques, lipofuscin, ceroid, and 'aggresomes' during oxidative stress, aging, and disease. Int J Biochem Cell Biol 2004, 36:2519–2530
77. Davies KJ: Protein damage and degradation by oxygen radicals. I general aspects. J Biol Chem 1987, 262:9895–9901
78. Halliwell B, Jenner P: Impaired clearance of oxidised proteins in neurodegenerative diseases. Lancet 1998, 351:1510
79. Lopiano L, Fasano M, Giraudo S, Digilio G, Koenig SH, Torre E, Bergamasco B, Aime S: Nuclear magnetic relaxation dispersion profiles of substantia nigra pars compacta in Parkinson's disease patients are consistent with protein aggregation. Neurochem Int 2000, 37:331–336
80. Rivett AJ: Preferential degradation of the oxidatively modified form of glutamine synthetase by intracellular mammalian proteases. J Biol Chem 1985, 260:300–305
81. Warso MA, Lands WE: Lipid peroxidation in relation to prostacyclin and thromboxane physiology and pathophysiology. Br Med Bull 1983, 39:277–280
82. Billings PC, Whitbeck JC, Adams CS, Abrams WR, Cohen AJ, Engelsberg BN, Howard PS, Rosenbloom J: The transforming growth factor-beta-inducible matrix protein (beta)ig-h3 interacts with fibronectin. J Biol Chem 2002, 277:28003–28009
83. Akhtar S, Meek KM, Ridgway AE, Bonshek RE, Bron AJ: Deposits and proteoglycan changes in primary and recurrent granular dystrophy of the cornea. Arch Ophthalmol 1999, 117:310–321
84. Zinn K, McAllister L, Goodman CS: Sequence analysis and neuronal expression of fasciclin I in grasshopper and Drosophila. Cell 1988, 53:577–587
85. Clout NJ, Tisi D, Hohenester E: Novel fold revealed by the structure of a FAS1 domain pair from the insect cell adhesion molecule fasciclin I. Structure 2003, 11:197–203
86. Karlsson K, Marklund SL: Binding of human extracellular-superoxide dismutase C to cultured cell lines and to blood cells. Lab Invest 1989, 60:659–666
87. Karlsson K, Sandstrom J, Edlund A, Marklund SL: Turnover of extracellular-superoxide dismutase in tissues. Lab Invest 1994, 70:705–710
88. LeBaron RG, Bezverkov KI, Zimber MP, Pavelec R, Skonier J, Purchio AF: Beta IG-H3, a novel secretory protein inducible by transforming growth factor-beta, is present in normal skin and promotes the adhesion and spreading of dermal fibroblasts in vitro. J Invest Dermatol 1995, 104:844–849